

PAPER

Plasma properties in the vicinity of the last closed flux surface in hydrogen and helium fusion plasma discharges






To cite this article: M Dimitrova *et al* 2024 *Plasma Phys. Control. Fusion* **66** 075022

View the [article online](#) for updates and enhancements.

You may also like

- [Contribution of joint experiments on small tokamaks in the framework of IAEA coordinated research projects to mainstream fusion research](#)
M GRYAZNEVICH, J STÖCKEL, G VAN OOST *et al.*
- [Remote operation of the GOLEM tokamak with hydrogen and helium plasmas](#)
V Svoboda, A Dvornova, R Dejarnac *et al.*
- [Contribution to fusion research from IAEA coordinated research projects and joint experiments](#)
M. Gryaznevich, G. Van Oost, J. Stöckel *et al.*

Plasma properties in the vicinity of the last closed flux surface in hydrogen and helium fusion plasma discharges

M Dimitrova^{1,*} , D López-Bruna² , J P Gunn³, J Kovačič⁴ , V Svoboda⁵, J Stockel^{5,6}, P Ivanova¹, E Vasileva¹, E Hasan¹, R Dejarnac⁶, U Losada⁷ , C Hidalgo²  and Tsv K Popov¹

¹ Emil Djakov Institute of Electronics, Bulgarian Academy of Sciences, 72, Tsarigradsko Chaussee, 1784 Sofia, Bulgaria

² Laboratorio Nacional Fusión, CIEMAT, Complutense 40–28040, Madrid, Spain

³ CEA, IRFM, F-13108 Saint-Paul-Lez-Durance, France

⁴ University of Ljubljana, Faculty of Mechanical Engineering, Aškerčeva cesta 6, SI-1000 Ljubljana, Slovenia

⁵ Faculty of Nuclear Sciences and Physical Engineering, CTU Prague, CZ-11519, Czech Republic

⁶ Institute of Plasma Physics of the Czech Academy of Sciences, U Slovanky 2525/1a, 182 00 Prague 8, Czech Republic

⁷ Auburn University, Auburn, AL, United States of America

E-mail: miglana.dimitrova@gmail.com

Received 12 January 2024, revised 22 May 2024

Accepted for publication 3 June 2024

Published 12 June 2024



CrossMark

Abstract

The origin of the bi-Maxwellian electron energy distribution function (EEDF) observed in the scrape-off layer (SOL) of tokamak plasmas by means of Langmuir probes is still under discussion. It has been assumed that the ionization of hydrogen and deuterium neutrals by thermal electrons penetrating the SOL from the bulk plasma is the main reason for the appearance of a second Maxwellian. To validate this assumption, radial measurements of the electron temperatures and densities, or the plasma properties in helium plasmas in the GOLEM tokamak and the TJ-II stellarator were performed. The radial profiles of the low-temperature electron group densities follow the trend of the calculated radial profiles of the electron sources arising from the ionization of neutrals in both deuterium and helium plasmas in TJ-II. The difference in the radial location where the bi-Maxwellian EEDF appears can be explained by the difference in the rate coefficients for ionization of deuterium and helium. The results of probe measurements in GOLEM and the WEST tokamak divertor, at one radial location in the SOL, are compatible with the hypothesis concerning the ionization of neutral atoms and the type of the EEDF.

Keywords: helium, ionization of neutral atoms, electron temperature, plasma diagnostics–probes

1. Introduction

The assumption of a Maxwellian electron energy distribution function (EEDF) in fusion plasmas is generally valid. However, there exist theoretical predictions [1–3]

and experimental evidence in tokamaks such as CASTOR, COMPASS, NXTS, J-TEXT, and TJ-II stellarator [4–7] suggesting the presence in some cases of non-Maxwellian distributions of the electrons in the vicinity of the last closed flux surface (LCFS) in fusion devices, namely, together with thermal electrons with energies in the range 10–30 eV, there is a low-temperature electron group with energies 5–7 eV. It has been shown in series of experiments on radial measurements

* Author to whom any correspondence should be addressed.

of the electron temperatures and densities in hydrogen and deuterium plasmas in different tokamaks, CASTOR [4], COMPASS [5], and ISSTOK [8], as well as in the TJ-II stellarator [5], that this non-Maxwellian EEDF can be approximated by a sum of two Maxwellian distributions, i.e. a bi-Maxwellian EEDF.

The origin of the bi-Maxwellian EEDF is still under discussion. In our previous work [5], we assumed that the ionization of hydrogen and deuterium neutrals by thermal electrons penetrating from the bulk plasma into the SOL is the main reason for the EEDF deviating from a Maxwellian: the ionization processes provide a population of cold electrons. In the present work we take this assumption as a working hypothesis. Since the ionization energy for deuterium and helium is different, and for deuterium it was confirmed that the appearance of the bi-Maxwellian EEDF requires electron temperatures around 13.6 eV [9], a way to check the validity of our hypothesis is to repeat the measurements in helium plasmas, where it is expected that the non-Maxwellian EEDF will appear when the electrons have an energy above the value for ionization for helium, around 24.5 eV. In this work, we present radial measurements of the electron temperatures and densities in helium plasmas in the GOLEM tokamak [10], the TJ-II stellarator [11] and in the divertor of the WEST tokamak [12].

A necessary verification is that the appearance of the cold-electron group and its density profile are compatible with the radial locations where the ionization source of electrons is significant. The calculations are performed using the EIRENE code in both deuterium and helium plasmas of the TJ-II device. The differences in the positions of appearance of a bi-Maxwellian EEDF can be explained by the differences in the rate coefficients for ionization of deuterium and helium [9].

The first probe measurements results in the WEST tokamak divertor tend to confirm the hypotheses of the ionization of neutral atoms and the type of the EEDF. There the experiments were connected to study also a mixture of deuterium and helium. It was found that the amount of the helium was very important for the change of the EEDF.

The aim of the article is to confirm the working hypothesis proposed in [5] using helium gas in different fusion devices. In section 2, there is a review of the main used technique applied on probes data. The advantage of the first-derivative probe technique (FDPT) is that it can give an information about the EEDF. Then, in section 3 are the experimental result from the probes including measurements in hydrogen and helium discharges of the GOLEM tokamak, measurements in deuterium and helium discharges in the TJ-II stellarator and the one of the divertor probes on WEST tokamak. A discussion of the results is provided in section 4 and the last section presents the conclusions.

2. First-derivative probe technique for evaluating the EEDF

The EEDF can be determined using current–voltage (I – V) probe characteristic applying the first derivative probe

technique [4]. The main points of the technique used in magnetized plasma are described below.

The classical Langmuir probe technique used to evaluate the isotropic part of the EEDF, $F(\varepsilon)$, from the measured I – V characteristic in a homogeneous gas-discharge plasma is relatively simple; however, to obtain reliable results, a number of conditions have to be satisfied [13, 14]: Immersed in the plasma, the probe disturbs it, with this disturbance being localized in the probe sheath. To obtain information on the EEDF in the non-disturbed plasma, the electrons originating from the undisturbed plasma should not change their energy when crossing the probe sheath and reaching the probe. This means that the mean free paths of the electrons and ions should be much larger than the size of the area disturbed by the probe $R_d = R + d$ (R being the probe radius and d , the probe sheath thickness), and they should reach the probe surface without collisions. This requires that the probe should be operated at very low gas pressures and in the absence of or in a very weak magnetic field, when the electron mean free path λ and the Larmor radius R_L are larger than R_d . Then, to obtain the EEDF one can use the well-known Druyvesteyn formula [15] expressing the proportionality between the second derivative of the I – V measured and the EEDF.

Swift [16] was the first to take into account the probe size and the effect of collisions in the probe sheath in evaluating the EEDF at non-negligible gas pressures. He pointed out that the second derivative of the I – V probe characteristic is distorted due to the depletion of electrons sinking into the probe surface.

The FDPT [17, 18] was developed on the basis of the non-local kinetic theory [19] in view of obtaining the EEDF in gas discharges at higher gas pressures (above 10 mbar) when the problem arises of the electron energy relaxation as the electrons cross the probe sheath in a diffusion regime. The energy relaxation length is defined by [20]:

$$\lambda_\varepsilon \approx 2 \left(\frac{D_e}{\nu_{ee} + \nu_{ea} + \nu^*} \right)^{1/2}. \quad (1)$$

Here ν_{ee} , ν_{ea} and ν^* are the electron–electron, electron–neutral and inelastic collisions rates; $\delta = m/M$; m and M are the electron and neutral masses, respectively. $D_e = v\lambda_e/3$ is the diffusion coefficient and λ_e is the mean free path of electrons.

The energy relaxation length is the basis of the non-local regime of probe operation, namely, if

$$\lambda_\varepsilon \gg R_d \gg \lambda_e, \quad (2)$$

then one can obtain information for the EEDF from the I – V measured. The above inequality means that the electrons reach the probe surface in a diffusion regime without energy relaxation.

The electron probe current density may be found by solving the Boltzmann kinetic equation for the isotropic part of the electron energy probability function (EEDF), $f_0(\varepsilon) = F(\varepsilon)/\sqrt{\varepsilon}$, which takes the form of the diffusion equation [18]:

$$\nabla_r D(W) \nabla_r f(W, r) = 0 \quad (3)$$

$W = mv^2/2 + e\phi(r)$ is the total electron energy and $\phi(r)$ is the potential distribution introduced by the probe. The diffusion coefficient in the non-local approach is $D(W) \equiv \nu D = \frac{v^2 \lambda_e}{3}$.

As shown [18] for a thin probe sheath, the electron probe current density in the case of $W \geq eV$ (V being the probe potential) is

$$j_e(U) = \frac{8\pi e}{3m^2 \gamma_0} \int_{eV}^{\infty} \frac{(W - eV) f(W) dW}{1 + \frac{(W - eV)}{W} \psi(W)}, \quad (4)$$

where $\psi(W)$ is the diffusion parameter:

$$\psi(W) = \frac{1}{\lambda_e(W) \gamma_0} \int_0^R \frac{D(W) dr}{(r/R)^n D(W - e\phi(r))}. \quad (5)$$

Here $n = 1$ for a cylindrical probe, $n = 0$ for a flat probe and $n = 2$ for a spherical probe. The value of the geometric factor γ varies monotonically from 0.71 to 4/3: $\gamma = 4/3$ when $\lambda, R_L \gg R + d$ and $\gamma = 0.71$ when $\lambda, R_L \ll R + d$.

The integral for $\psi(W)$ is divergent so that the upper limit is taken to be the length of the probe L . When $\psi(W) \gg 1$, the EEPF is not represented by the Druyvesteyn formula, but rather by the first derivative of the electron probe current:

$$f(\varepsilon) = \frac{3\sqrt{2m}}{2e^2 S} \frac{\psi}{eV} \frac{dI_e}{dV}. \quad (6)$$

At the end of the work of Arslanbekov *et al* [18] briefly, without experimental confirmation, the extension of the applicability of the FDPT to magnetized plasma is presented.

For magnetized plasma, the length of energy relaxation has two components—along and across the magnetic field:

$$\lambda_{\parallel}^{\parallel} = \lambda_{\varepsilon} \text{ and } \lambda_{\varepsilon}^{\perp} = \lambda_{\varepsilon} / \alpha \quad (7)$$

where for homogeneous plasma $\alpha = \left[1 + (\lambda_e/R_L)^2\right]^{1/2}$.

In such a case, the diffusion coefficient $D(W)$ becomes a tensor with two components:

$$D_{\parallel}(W) = \frac{v^2 \lambda_e(W)}{3}; \quad D_{\perp}(W) = D_{\parallel}(W) / \alpha^2 \quad (8)$$

and the diffusion equation for a magnetic field oriented along the z axis is:

$$D_{\perp}(W) \Delta_r f_0 + D_{\parallel}(W) \Delta_z f_0 = 0. \quad (9)$$

The solution of this equation is sought for a probe considered as an ellipsoid of revolution with dimensions R and $b = L/2$. In elliptic coordinates for a probe placed along the magnetic field, this yields for the diffusion parameter:

$$\psi_{\parallel}(W) = \frac{S\alpha}{8\pi \beta_{\parallel}^M \lambda(W) \gamma} \ln \left(\frac{\sigma_{\parallel}^M + 1}{\sigma_{\parallel}^M - 1} \right) \quad b' > R \quad (10)$$

$$\psi_{\parallel}(W) = \frac{S\alpha}{8\pi \beta_{\parallel}^M \lambda(W) \gamma} \left(\pi - 2 \arctan \sigma_{\parallel}^M \right) \quad b' < R,$$

where $\beta_{\parallel}^M = \left(|R^2 - b'^2| \right)^{1/2}$, $b' = \frac{b}{\alpha}$, $\sigma_{\parallel}^M = \frac{b'}{\left(|R^2 - b'^2| \right)^{1/2}} = \frac{b'}{\beta_{\parallel}^M}$.

For a probe placed across the magnetic field, the diffusion parameter is found to be:

$$\psi_{\perp}(W) = \frac{S\alpha}{4\pi \beta_{\perp}^M \lambda(W) \gamma} F(\varphi/\beta), \quad (11)$$

where $F(\varphi/\beta)$ is an incomplete elliptical integral of the first kind and

$$\begin{aligned} \beta_{\perp}^M &= \left(|R^2 - b^2| \right)^{1/2} \quad R' = \frac{R}{\alpha} \cos(\varphi) = \frac{a}{b} \cos(\beta) \\ &= \frac{(R^2 - R'^2)}{\beta_{\perp}^M}. \end{aligned}$$

These equations were applied to the diagnostics of a linear gas discharge [21] with magnetic fields in the range 0.015–0.08 T and showed that for $\psi(W) \sim 1$, an extended Druyvesteyn formula [22] should be used. At $\psi(W) \gg 1$, the FDPT provides reliable results for the EEDF. Both techniques (the first derivative probe technique and the technique based on the extended Druyvesteyn formula) can be applied to obtain the EEDF in argon magnetized gas discharges by perpendicular probe in the magnetic field range of 0.045–0.075 T [19].

Chronologically, Demidov [20, 23] was the first to use the results of the probe theory in a non-local approach for systematic evaluation of the EEDF in the ‘Blaamann’ device [24] in the presence of higher magnetic fields up to 0.4 T in helium gas discharges at gas pressures from 0.03 to 0.3 Pa. In this device a weakly ionized plasma is produced by electrons accelerated from a hot negatively biased tungsten filament, the magnetic field is on z axis.

Although the global transport of the charged particles for the typical experimental conditions in the ‘Blaamann’ device was shown to be anomalous due to large-scale electrostatic fluctuations [24], the solution of the diffusion equation (9) was sought in a regime of classical electron transport to the probe [23], where the perpendicular diffusion is expressed by the parallel one using the relation $\frac{D_{\perp}}{D_{\parallel}} = \frac{1}{\eta^2}$:

$$\begin{aligned} \frac{1}{\eta^2} [\nabla_x (D_{\parallel}(W) \nabla_x f_0) + \nabla_y (D_{\parallel}(W) \nabla_y f_0)] \\ + \nabla_z D_{\parallel}(W) \nabla_z f_0 = 0 \end{aligned} \quad (12)$$

where

$$\eta = \left[1 + \frac{\omega_H^2}{(\nu_a + \nu_e)} \right]^{1/2} = \left[1 + \frac{\lambda_e(W)^2}{R_L(W, B)^2} \right]^{1/2}. \quad (13)$$

The non-locality condition is $\lambda_e (R_L/\lambda_e) \gg R_d \gg R_L$ [25].

For a magnetic field of 0.3 T and a gas pressure of 0.2 Pa, $\eta \approx \frac{\lambda_e}{R_L}$ and $\frac{D_{\perp}}{D_{\parallel}} \ll 1$. It is clear that the first term in the diffusion equation (12) has then a negligible contribution and the electrons are collected mostly in a direction parallel to the magnetic field lines.

The solution for the electron probe current is the same as in [18], equations (4) and (5). As it was mentioned, with infinity as the upper limit the integral for $\psi(W)$ is divergent. The region from which electrons are drawn to the probe is considered as an ellipsoid. Then the upper limit of the integral can be chosen as being the length of a flux tube from which the electrons are collected with equal fluxes in parallel and perpendicular directions [26]. For a probe perpendicular to the magnetic field, it is $R \ln(\pi L/4R)\eta$; and for a parallel probe, $\pi L\eta/4$. For $\gamma = 1$ and assuming $D(W) \approx D(W - e\phi(r))$, one finds:

$$\psi_{\perp}(W, B) = \frac{R \ln(\pi L/4R)}{R_L(W, B)}. \quad (14)$$

For a probe parallel to the magnetic field, the diffusion parameter $\psi_{\parallel}(W, B)$ is:

$$\psi_{\parallel}(W, B) = \frac{\pi L}{4R_L(W, B)}. \quad (15)$$

Under the conditions considered in this work, both the parallel and the perpendicular $\psi_{\parallel, \perp}(W, B)$ are much larger than unity, so that the EEPF is proportional to the first derivative of the electron probe current (equation (6)). The results obtained were summarized in the review article [25]. The Arslanbekov and Demidov's approaches consider a homogeneous plasma and cannot be applied to probe measurements in fusion plasmas with strongly turbulent and strongly magnetized ($B \sim 1-4$ T) edge and scrape-off layer (SOL). Moreover, in a highly turbulent plasma, the drift motion of charged particles acquires a random character. Electrons drifting in randomly varying fields are subject to shifts, whose magnitude and direction change randomly in space and time. Thus, their trajectories become quite similar to the trajectories observed in the cases of elastic collisions. Therefore, an effective collision rate, ν_e^{eff} , respectively an effective electron free path, λ^{eff} , are introduced [27]. In such a case, the Bohm diffusion appears more widely applicable and thus $\nu^{\text{eff}} = 1/g\omega_L$, or $\lambda^{\text{eff}} = gR_L$, where the coefficient $g = 16$ is defined empirically [27]. The effective rate of the collisions determining the anomalous diffusion is much higher than the real rate of collisions of electrons with heavy particles [27, 28].

Regarding the probe measurements in fusion plasma, the non-locality condition $\lambda_e (R_L/\lambda^{\text{eff}}) \gg R_d \gg \lambda^{\text{eff}}$ is satisfied and $\frac{D_{\perp}^{\beta}}{D_{\parallel}^{\beta}} = \frac{1}{\beta^2} = \frac{1}{16} \frac{R_L}{\lambda^{\text{eff}}} = \frac{1}{16^2}$. Again, the first term in the diffusion equation (12) has a negligible contribution and one can get the same equations for the electron probe current (equation (4)) and for the diffusion parameter (equation (5)).

The estimation of the upper limit A in the integral for $\psi_{\parallel, \perp}(W, B)$

$$\psi_{\parallel, \perp}(W) = \frac{1}{\lambda^{\text{eff}}\gamma_0} \int_R^A \frac{D(W)dr}{(r/R)^n D(W - e\phi(r))} \quad (16)$$

needs a more detailed discussion. For a homogeneous plasma with a straight and constant magnetic field, the cross-sectional shape and area of the magnetic flux tube subtended by the probe remain constant. However, this is not the case in the tokamak edge and SOL, even if the turbulences are not considered [29]. On the other hand, the turbulent structures are crossing the probe area much faster than the probe potential changes (in fusion experiments, the probe is usually biased by a triangular potential at frequencies of 500 Hz–1 kHz [14]); this is evidenced by the fluctuations of the ion-saturation probe current.

It thus becomes clear that one cannot estimate theoretically the length of the ellipsoid from which electrons are drawn to the probe, as in the case of homogeneous plasma. Our solution to the problem is to compare our results with other methods and calibrate the values of the diffusion parameters $\psi_{\parallel, \perp}(W, B)$. First, we use a comparison with the three-parameter technique widely used in probe diagnostics of fusion plasma.

The three-parameter technique assumes a Maxwellian EEDF, but in fact does not measure the real one. The approximation for the probe current as a function of the probe potential, V_p around the floating potential, V_{fl} providing the value of the electron temperature is given by [29]:

$$I(V_p) = I_s^i \left\{ 1 - \exp \left[-\frac{e(V_{fl} - V_p)}{T_e} \right] \right\}. \quad (17)$$

The electron density can be found from the ion-saturation current value $I_s^i = 0.5en_e c_s A_p$, where A_p is the area of the probe projection in the direction of the magnetic field \vec{B} , and $c_s = [e(T_e + T_i)/m_i]^{1/2}$ is the ion acoustic velocity; T_e and T_i are the electron and ion temperatures in eV. Close to the LCFS, where we found two electron populations—a low-energy group and higher-energy thermal electrons, one has to use the effective electron temperature $T_e^{\text{eff}} = \frac{T_e^h T_e^l (n_e^l + n_e^h)}{n_e^h T_e^l + n_e^l T_e^h}$ to calculate the ion acoustic velocity.

The difference between the plasma potential and the floating potential is given by:

$$V_p - V_{fl} = \frac{kT_e}{2e} \ln \left[2\pi \frac{m_e}{m_i} \left(1 + \frac{T_i}{T_e} \right) (1 - \delta)^{-2} \right], \quad (18)$$

where m_e and m_i are the electron and ion mass and δ is the coefficient of secondary electron emission.

The comparison between the results of the three-parameter technique and the first-derivative one shows a very good agreement between the estimated electron temperatures [5, 30]. Note that for a given magnetic field value B , to evaluate

the $f(\varepsilon)$ in arbitrary units (respectively the electron temperature) one does not need the actual values of $\psi_{||,\perp}(W,B) = \psi_{||,\perp}^0(B)/\sqrt{W}$, so that $f(\varepsilon) = \frac{\text{const } dI_e}{V\sqrt{V} dV}$.

At the same time, using Demidov or Arslanbekov's equations for $\psi_{||,\perp}(W,B)$ yields a discrepancy of one order of magnitude with the electron density as estimated by the three-parameter technique (using a reasonable value of the ion temperature).

The only solution for estimating the upper limit A in the integral for $\psi_{||,\perp}(W,B)$ was to empirically accept a value of about $L' \approx 0.1$ m, which is of the order of the turbulence vortices size. Thus, the length of the area from which the electrons are collected for a probe parallel to the magnetic field becomes $\pi L'/4$, and for a perpendicular probe, $R \ln(\pi L'/4R)$.

Then for a parallel probe with a thin probe sheath we arrive at [14, 31]

$$\psi_{||} = \frac{1}{\gamma\lambda^{\text{eff}}} \int_R^{\pi L'/4} \frac{dr}{(r/R)^0} \approx \frac{\pi L'}{4\gamma\lambda^{\text{eff}}} \approx \frac{\pi L'}{4\gamma 16R_L} = \frac{\pi L'}{64\gamma R_L(W,B)}. \quad (19)$$

For a perpendicular probe

$$\begin{aligned} \psi_{\perp} &= \frac{1}{\gamma\lambda^{\text{eff}}} \int_R^{R \ln(\pi L'/4R)} \frac{dr}{(r/R)^0} = \frac{R \ln(\pi L'/4R) - R}{\gamma\lambda^{\text{eff}}} \\ &\approx \frac{R \ln(\pi L'/4R)}{\gamma\lambda^{\text{eff}}} = \frac{R \ln(\pi L'/4R)}{\gamma 16R_L(W,B)}. \end{aligned} \quad (20)$$

These equations were used in our works to estimate the electron temperatures and densities and the plasma potential. In [31], we introduced an iterative procedure to obtain more accurate results.

The FDPT was successfully applied to the probe diagnostic experiments on the CASTOR [4], COMPASS [5, 30] and ISSTOK [8] tokamaks, as well as on the TJ-II stellarator [5] where examples are included how the T_e is determined. The EEPF obtained using our expressions for $\psi_{||,\perp}(W,B)$ in hydrogen and deuterium plasmas in the COMPASS tokamak and the TJ-II stellarator yielded values of the electron temperatures and densities in satisfactory agreement with the Thomson scattering (TS) results, as well as with the calculations by the ASTRA package for the COMPASS tokamak and by the EIRENE code for the TJ-II stellarator [5, 32].

3. Experimental results—Langmuir probe measurements

3.1. Measurements in hydrogen and helium discharges of the GOLEM tokamak

As mentioned in the Introduction, the hypothesis that a bi-Maxwellian EEDF appears in presence of neutrals and sufficiently hot electrons was proposed in [4, 5]. The ionization of

the neutral atoms is assumed responsible for the appearance of a cold-electron population. To confirm this, a series of experiments were performed in the simplest operating tokamak in the Czech Republic, namely, the GOLEM tokamak [10].

A probe used in a swept mode to measure the I - V characteristics was inserted from the bottom of the chamber and consisted of two 1 mm tungsten pins—parallel (having a length of 10 mm) and perpendicular (length of 3 mm) to the magnetic field lines. Figure 1(a) is a schematic of the GOLEM chamber cross-section; figure 1(b) shows a photograph of the probe head with the two pins. The measurements were carried out without a filter and the perpendicular probe measured ion saturation current, I_{sat} at -100 V. At each consecutive discharge, the probe head was moved more deeply into the plasma with the purpose of plotting radial profiles of the plasma parameters.

Figure 2 shows the main plasma parameters of the discharges in hydrogen (figure 2(a)) and helium (figure 2(b)) in the GOLEM tokamak. The discharges in helium were shorter, so that the data were processed at different times during the discharges—for hydrogen at $t_H = 21$ ms and in helium, at $t_{\text{He}} = 13$ ms shown by dashed lines in blue and red respectively. Our previous work [33] was dedicated to the importance of cleaning the vacuum chamber and the effect of the impurities, and explained the reason why the helium discharges were shorter, being more sensitive to impurities.

The I - V s acquired by the parallel probe were processed by using the FDPT. The determined radial profile of the electron temperature and density are shown in figure 3. It is seen that the T_e in helium plasma is 5–7 eV (red circles in figure 3(a)) and the EEDF is everywhere Maxwellian. In the case of hydrogen, the EEDF is also Maxwellian with temperature 7.5–9 eV in the region of the limiter (blue, empty circles in figure 3(a)), but in the confined plasma it can be approximated by a bi-Maxwellian EEDF with two groups of electrons, namely, a more populated one of cold electrons (4 eV, blue triangles) and thermal electrons (blue squares) with temperature around 14 eV. The accuracy of evaluating the temperature of the predominant cold electron fraction is $\sim 10\%$, while for the minority high-temperature electron population the uncertainty increases to $\sim 25\%$ due to its low density. Figure 3(b) shows the radial profiles of the electron densities. In the case of He plasma when the EEDF is Maxwellian, the results are presented by the empty red circles. In the case of H_2 , open blue circles present the Maxwellian EEDF, while for the bi-Maxwellian one, the electron densities are illustrated by the same symbols as used in figure 3(a) for the temperatures—triangles for the cold electrons and squares for the thermal electrons.

The power provided by the GOLEM tokamak is not sufficient to heat the electrons in the He discharges to temperatures exceeding 7 eV, so that the EEDF observed was Maxwellian. Since the expectations were that, for helium, the non-Maxwellian EEDF should appear when the electrons have an energy above the value for ionization for helium, around 24 eV, GOLEM experiments on helium are compatible with the working hypothesis but cannot confirm it.

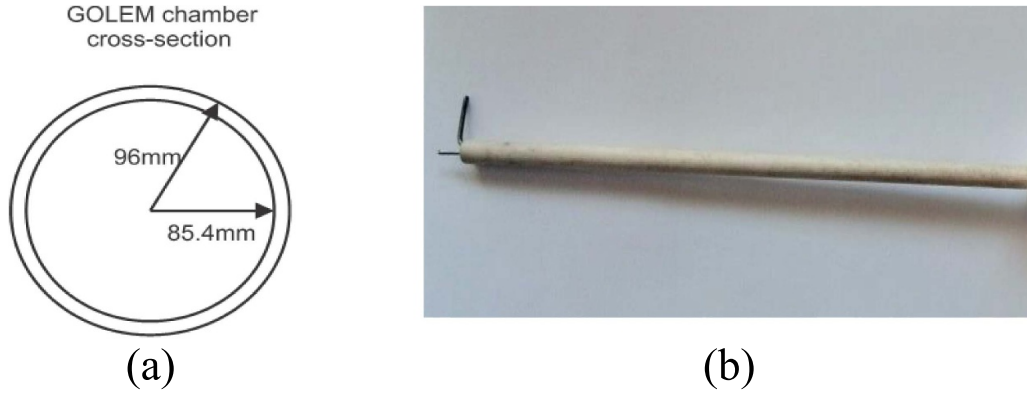


Figure 1. Schematic cross-section of the GOLEM tokamak chamber (a) and photograph of the probe head (b) with the two pins.

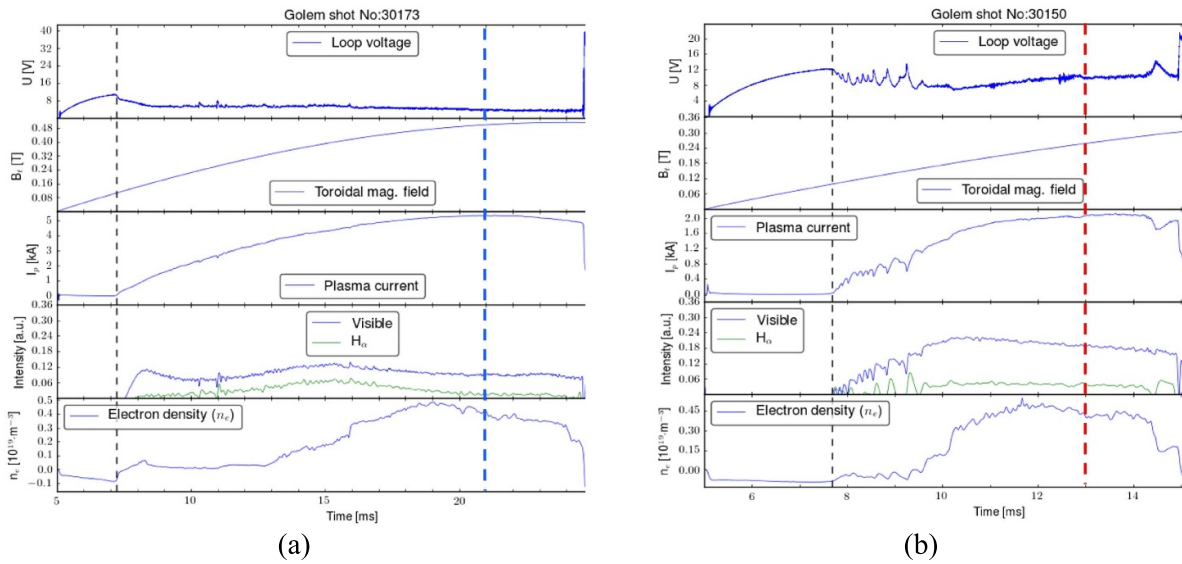


Figure 2. Main plasma parameters of the discharges in hydrogen (a) helium (b) in GOLEM tokamak.

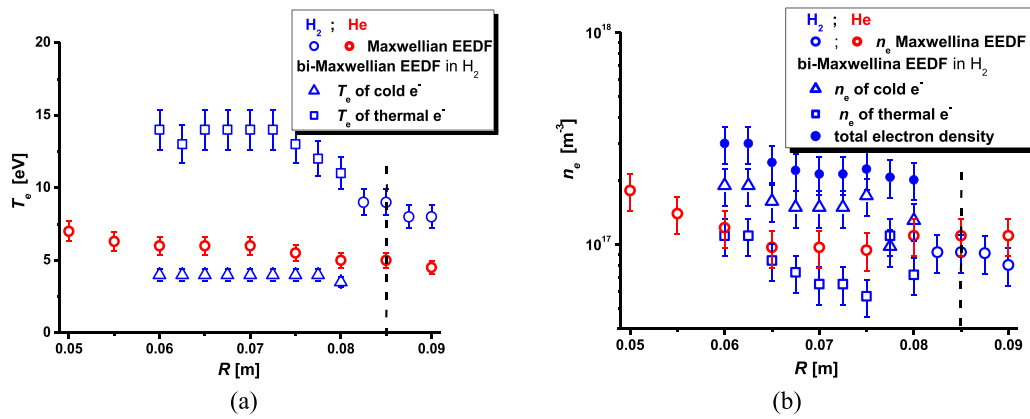


Figure 3. Radial measurements of the electron temperature (a) and electron density (b) for hydrogen (blue) and helium (red) discharges.

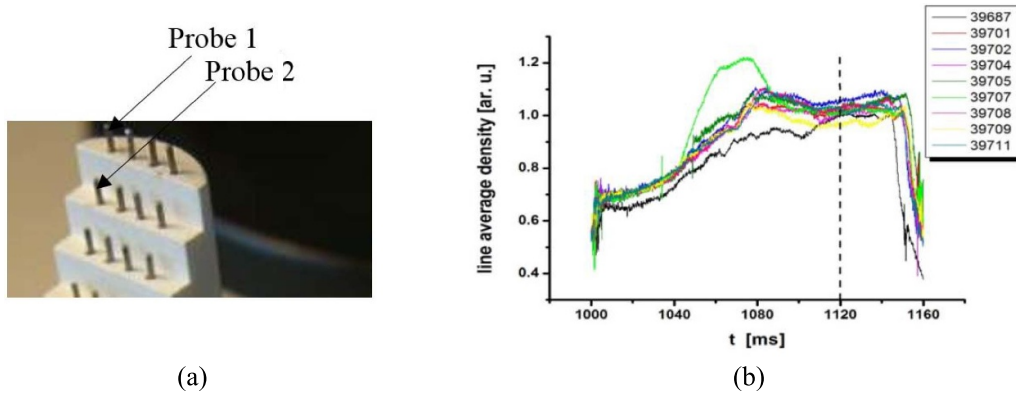


Figure 4. Probe head (a) used for the measurements on the TJ-II stellarator and line-average densities of the processed discharges (b).

In hydrogen discharges the electrons were hotter than 13 eV and a bi-Maxwellian EEDF is registered. In the limiter shadow, behind the poloidal ring limiter at 0.85 m, the EEDF was instead Maxwellian. These results are similar to the observations on CASTOR [4], ISTTOK [8] and COMPASS [5] tokamaks in hydrogen and deuterium plasmas.

It should be mentioned here, that another similar experiments were performed on GOLEM in helium plasma, using a perpendicular small Langmuir probe (length of 2 mm and diameter 0.7 mm). The determined highest temperature at the deepest position is 15 eV where the EEDF is still Maxwellian. To conclude, the experiments presented in this section were only partly successful.

3.2. Measurements in deuterium and helium discharges in the TJ-II stellarator

The results obtained during deuterium discharges in the TJ-II stellarator were published in [5]. We reported there that during neutral-beam injection (NBI) heating, the EEDF in the confined plasma and close to the LCFS is bi-Maxwellian, while in the far SOL the EEDF is Maxwellian. Thus, in this section we will only deal with helium discharges.

The helium experiment was performed in the TJ-II stellarator by a series of discharges with a magnetic field of 1 T and NBI heating. The probe head used is shown in figure 4(a). In the measurements discussed here, the first probe at the top (LP#1) and the first one in the second row (LP#2) were only used. The probes have a diameter of 0.75 mm and a length of 2.4 mm; the distance between them is 5 mm, oriented perpendicular to the magnetic field lines. They were inserted from the top of the TJ-II chamber (low-field side).

The discharges performed had practically identical line-average densities at the time of evaluation (1120 s), indicated by a dashed line in figure 4(b). The probes were moved more deeply into plasma with each successive discharge. During the data processing, when the diffusion parameter (equation (14)) has a low value, a second term is added to the FDPT (see [4], figure 3(a)). The results from the probe measurements in helium discharges on the TJ-II stellarator are presented below.

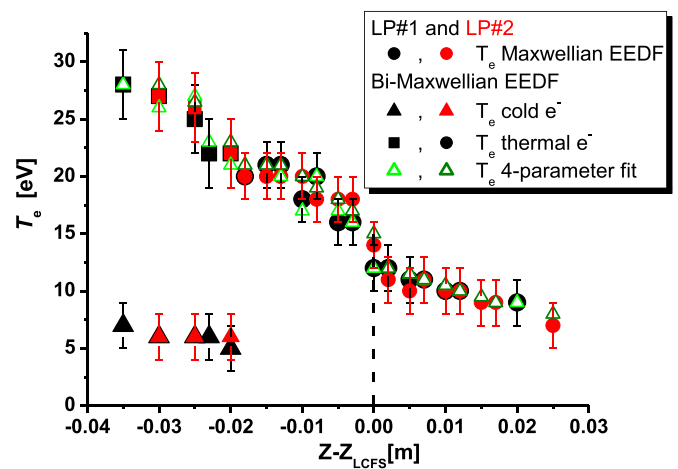


Figure 5. Radial distribution of the electron temperatures T_e acquired by LP#1 (black) and LP#2 (red) on the TJ-II stellarator, helium discharges. The triangles refer to the cold electrons of the EEDF obtained by using the FDPT; the squares, the thermal electrons; and the circles, the T_e of the Maxwellian EEDF. The empty, green triangles present the results obtained by the four-parameter technique.

The radial distribution of the electron temperatures obtained by using the FDPT are presented in figure 5 by circles, squares and triangles, black for LP#1 and red for LP#2. The solid triangles present the cold electrons of the EEDF in a case of bi-Maxwellian EEDF; the squares—the thermal electrons; and the circles, the T_e of the Maxwellian EEDF.

Because the ion part of the $I-V$ does not reach saturation, a sheath expansion takes place; it thus becomes necessary to use a technique that can take into account this linear change. The best technique is the four-parameter fit [34, 35] (empty, green triangles in figure 5), which we used to compare with the results obtained by using the FDPT. Using the four-parameter fit the I_{sat} and T_e and V_{fl} are determined, the fourth parameter (the derivative dI/dV) is to compensate the non-saturated slop in the ion branch of the $I-V$. In the case of non-Maxwellian EEDF, this techniques as the three-parameter one is sensitive only to the thermal electrons, because for the fit is used the ion

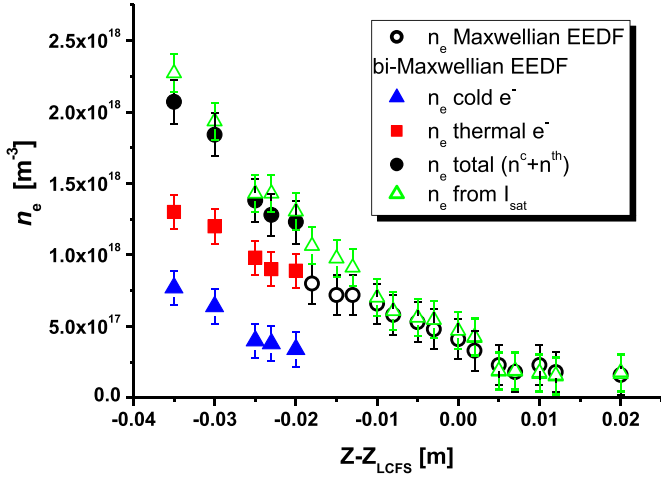


Figure 6. Radial distribution of the electron densities n_e acquired by LP#1 on the TJ-II stellarator, helium discharges. The blue triangles refer to the cold electrons of the EEDF obtained by using the FDPT; the red squares, the thermal electrons; and the circles, the n_e of the Maxwellian EEDF. The empty green triangles represent the plasma parameters obtained by the four-parameter technique.

branch and the vicinity of the floating potential of the I - V and assumes that the EEDF is Maxwellian.

Similar comparison applying different probe techniques to determine the plasma parameters was done on the example of H-mode measurements on the COMPASS tokamak [36]. The conclusion was that the four-parameter fit and the FDPT yield similar results for the plasma parameters, while the three-parameter fit [29] (equation (17)) overestimates I_{sat} and T_e .

In a Maxwellian case, the electron temperatures obtained by the two techniques coincide. In the case of a bi-Maxwellian EEDF, the data from the four-parameter fit are strongly influenced by the high-energy tail of the electron energy distribution.

The radial distribution of the electron density obtained by using the FDPT is shown in figure 6. Only the LP#1 results are presented, because LP#2 is shadowed and measures slightly lower I_{sat} and n_e . The blue triangles indicate the cold electrons of the bi-Maxwellian EEDF; the red squares, the thermal electrons; and the circles, the n_e of the Maxwellian EEDF. The empty green triangles represent the plasma parameters obtained by the four-parameter technique, which agree with the sum of the densities of both groups of electrons- the cold, n_e^c and the thermal, n_e^{th} , in the case of bi-Maxwellian EEDF.

Concerning the ion temperatures, necessary for the calculations that lead to the data in figures 5 and 6, the data are the same as those used for the calculations of the EIRENE code. Since T_i is not measured in TJ-II in the SOL (positive $Z-Z_{\text{LCFS}}$), a constant ion temperature of 18 eV is assumed in the vicinity of the LCFS.

It should be noted that the probe measurements on the TJ-II stellarator during the NBI phase in helium discharges yield similar results for the electron temperatures T_e and densities n_e as in deuterium discharges published in [5]. The differences in the plasma properties now are at the temperature when

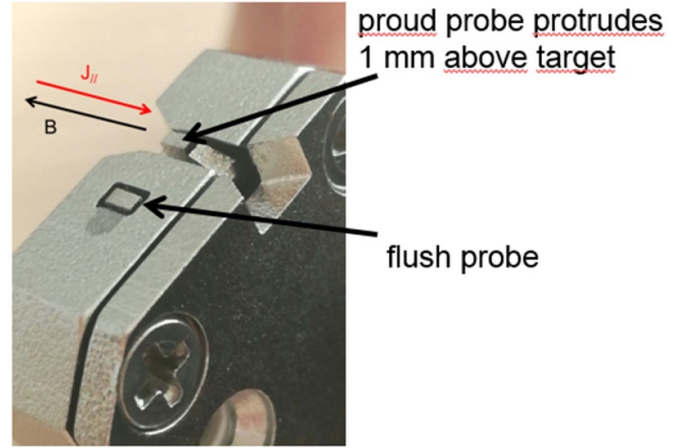


Figure 7. Mousetrapped probe head.

the splitting starts: figure 5 shows that, in the vicinity of the LCFS and in the far SOL, the EEDF is Maxwellian with temperatures 9–20 eV. In the region deeper than 20 mm inside the confined plasma, where the electron temperature exceeds 21 eV, the EEDF is bi-Maxwellian and the profile is split into two branches with cold electrons (triangles) with a density lower than the thermal electrons (squares). We recall that, in deuterium [5], a bi-Maxwellian EEDF appears in the SOL, around 4 mm off the LCFS, with T_e exceeding 12 eV and the cold population exceeding the hot one.

3.3. Measurements on the divertor of the WEST tokamak

On 14 December 2016, the WEST tokamak, CEA, Cadarache [12], France, produced its first plasma. A magnetically driven ‘mousetrap’ probe head (figure 7) equipped with a flush-mounted probe and a classical ‘proud’ probe with a well-defined collecting area was installed in the lower divertor. In an experiment with different amounts of helium in the discharges, the flush probe was used to measure the I - V characteristics. The radial position of the mousetrap probe corresponds to the radial position of the divertor probe #29 (again flush-mounted probe but of bigger size, a flat, circular probe of diameter 2.5 mm) [37], which allows for a good comparison of the results. The typical outer strike point (OSP) position on WEST is on divertor probe #25, it means that mousetrap probe is around 5 cm in the outer divertor with respect to the OSP.

The probes were swept by a 500 Hz triangular voltage ($-180 \div +80$ V). The flush-mounted probes have a problem with the effect of sheath expansion on the ion-saturation current I_{sat} that is why again the four-parameter fit was used to process the I - V characteristics. The FDPT is not sensitive to the not saturated ion-part and is applied mainly to determine the EEDF. A series of identical discharges are performed where only the ratio between the deuterium and helium is different. The isotope ratio is determined by means of threshold ionization mass spectrometry (TIMS) using the signal of residual gas analysers [38]. As an example, figure 8 presents the results from measurements in L-mode discharges

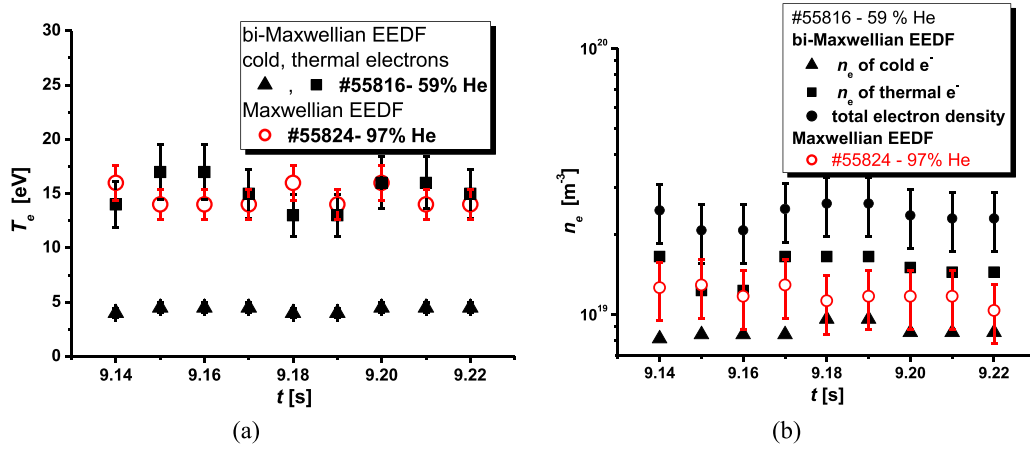


Figure 8. Temporal distribution of the electron temperatures T_e (a) for 59% (black) and 97% (red) of He and the corresponding electron densities n_e (b) measured by the flush probe on the mousetrap head.

#55824 (97% He/(He + D₂)) and #55816 (59% He/(He + D₂)) with plasma current $I_{pl} = 0.3$ MA and line average density $n_e^{avr} = 3 \times 10^{19} \text{ m}^{-2}$, toroidal magnetic field was $B_T = 3.7$ T.

Figures 8 (a) and (b) show the temporal profiles of the electron temperature and the electron density during the period (9.13–9.23 s) when the probe is inserted to the plasma and measures I - V_s . It is seen that in the discharge with a higher amount of He (red symbols), the EEDF is Maxwellian. In the case of the discharge with less helium (59%, black symbols), together with thermal electrons with temperatures $T_e^h = 13 \div 17$ eV there appears a group of cold electrons with $T_e^l = 4 \div 4.5$ eV. The corresponding electron densities show that the more populated electrons are the thermal (black squares in figure 8(b)), which are almost twice more than the cold electrons (black triangles). This finding is similar to the observed in the TJ-II stellarator in the confined plasma close to the LCFS.

The origin of the cold electron population is discussed in detail in [5], where it is shown that the main reason of this phenomenon is intensive ionization of the deuterium neutrals by thermal electrons in the vicinity of the LCFS. As a result of the ionization the cold electrons are born. Analyzing the discharges with different amount of He it was found that below 80% the EEPF is always bi-Maxwellian, at 82% of He, #55825 appears Maxwellian distribution with $T_e = 13 \div 15$ eV. It means that the deuterium in the gas mixture with He still plays important role for the ionization and is the reason for the non-Maxwellian EEDF. In the gas mixture when the deuterium is still good amount the ionization process is going mainly through it and less via helium. In the pure He the temperature of the thermal electrons is not sufficiently high to observe a bi-Maxwellian distribution. The four-parameter fit give very similar T_e , corresponding to the thermal electrons in the case of bi-Maxwellian EEDF.

These first results show that the EEDF in the case of an almost pure He plasma is usually Maxwellian with a T_e around 17 eV; in contrast, with less He the working gas is deuterium and the EEDF can be non-Maxwellian. The comparison between the results acquired by the flush probe

on the mousetrap head and the divertor probes shows a good agreement. The results of calculating the electron density by the technique (FDPT) depend on the value of an integral derived using the kinetic diffusion theory taking into account the effect of the magnetic field on the mean free path. The independent cross-check with the ion density calculated by the classical probe theory shows a correct trend. As in the case of the experiments performed on the GOLEM tokamak, the temperature of the He plasma is not sufficiently high to observe a bi-Maxwellian distribution – production of electrons requires that the electron temperature be near He ionization potential.

4. Discussion

In this section, the main discussion is on the results obtained on the TJ-II stellarator. The EIRENE code is used in view of enabling a comparison with the results quoted in [5] for deuterium discharges, namely, the output of the code calculations for the electron sources of ionization S_e is compared with the experimental data. If the cold population in the bi-Maxwellian EEDF is due to ionization processes, the density of such cold population is expected to be linearly related with the electron source density, S_e , due to helium ionization, as long as the thermal electron energy is high enough.

The calculations of S_e were performed assuming pure He plasma. The experiments were done on TJ-II discharges started by hydrogen-NBI on a background of helium neutrals without further gas puffing. This can be done operating the device with Li-coated walls [39], where the recycling is very low for hydrogen but very high for helium: H⁺ ions produced by the NBI react with the Li covering the TJ-II chamber and create a solid compound with them. Since the plasmas reached an electron density plateau (figure 4(b)) during NBI injection, it can be assumed that these were essentially helium plasmas. The input electron density and temperature profiles were taken from an average of TS profiles at the time of interest (vertical dashed line in figure 4(b)), combined with lithium-beam data near the edge.

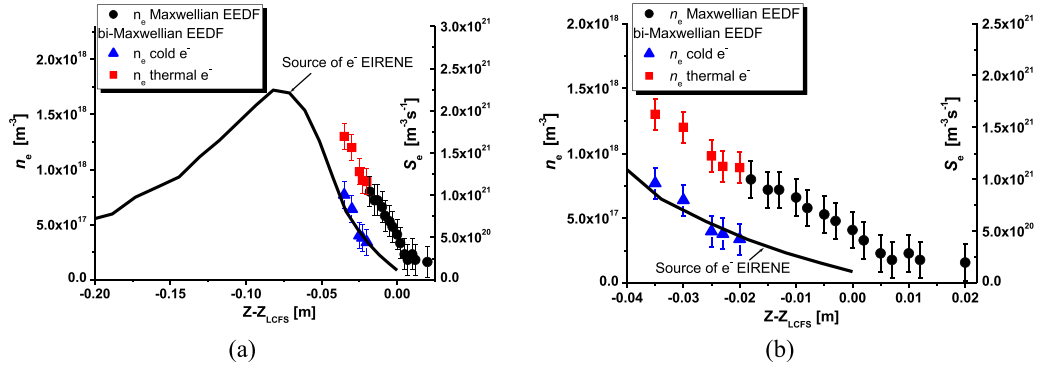


Figure 9. (a) Comparison between the radial distribution of the electron source S_e (solid line) calculated by EIRENE code and the experimental electron densities for NBI heating of He discharge in the TJ-II stellarator; (b) expanded view of the region around the LCFS.

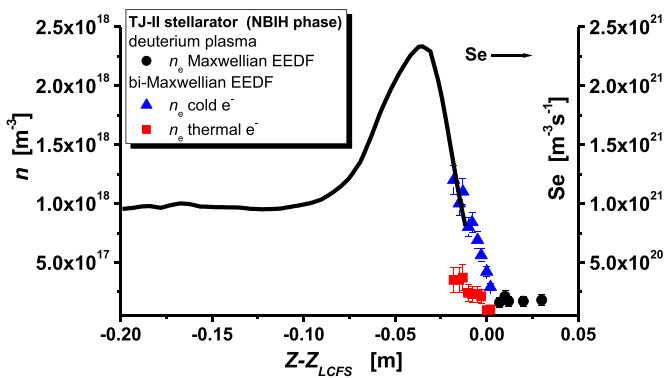


Figure 10. Comparison between the radial distribution of the electron source S_e (black line) calculated by EIRENE code and the experimental electron densities for NBI heating of deuterium discharge in the TJ-II stellarator. See figure 17 from [5]. Reproduced from [5]. © 2015 EURATOM.

EIRENE calculations for TJ-II provide 3D distributions of the output magnitudes. In particular, we have obtained the electron source density by helium ionization along the chord followed by the probe (figure 9). In this way, the calculated S_e can be compared with the densities of the thermal and cold temperature populations obtained with the FDPT. Figure 9(b) presents an enlarged view of the LCFS region, where the trend of the cold population clearly follows the intensity of the source.

In figure 10 we recall the same comparison between the electron source S_e profile and the electron densities already published in [5]. As in figure 9(b), here the cold electron component appears where the values of the calculated source-density curve are around $5 \times 10^{20} \text{ m}^{-3} \text{ s}^{-1}$, despite the different cold-electron densities in both cases.

The relatively larger population of cold electrons in deuterium should also conform with the hypothesis that they are due to the ionization of neutrals. Figure 11(a) shows the radial distribution of atomic neutrals, according to the calculations, for a deuterium discharge (blue squares) and a helium discharge (red squares).

Figure 11(b) presents the calculated electron source profiles in discharges with D_2 (blue) and He (red) filling gas. The blue line in figure 11(b), corresponding to D_2 , is the same as the one on figure 10 and the one published in [5]. For comparison, the new results show that the maximum of S_e for He appears more deeply in the plasma than for D_2 . The probe measurements were performed in the region of the rectangles ($\pm 0.035 \text{ m}$ in figure 11(b)), where the EEDF is changed from Maxwellian to bi-Maxwellian at the locations shown in the same figure by the sign (o, circle) in blue for D_2 and in red for He. Figure 11(b) is then compatible with having a comparatively large population of cold electrons in the deuterium case.

Note that the radial profile of the electron source is only calculated in the plasma region. Figure 11(a) informs that the atomic-neutrals density near the LCFS is very significant in both types of plasma. The larger source term in D_2 is due to the contribution from molecular deuterium, which outnumbers by about one order of magnitude the atomic deuterium density near the LCFS [32]. At the same time, however, the cold population densities follow the trend of the electron sources in the confined plasma, not the neutral densities. This is again consistent with the statement that the main reason for bi-Maxwellian EEDF observed in the vicinity of the LCFS is the ionization of neutral atoms.

As mentioned, for the case of He discharges the densities of the cold electrons are lower than those of the thermal group. In deuterium the situation is opposite. In order to discuss this fact, we first note two differences between H_2 and He cases: the much higher He neutrals density (about 16 times higher than for H_2 case; see figure 11(a) and the difference in the ionization rate coefficients of He and H_2 (shown in figure 12). The ionization rate of H_2 is an order of magnitude higher than that of He around 10 eV. Since the ionization rate coefficients for both gasses is at the dashed line level in figure 12 ($5 \times 10^{-9} \text{ cm}^3 \text{ s}^{-1}$), then one has to expect that the bi-Maxwellian EEDF in He appears above 21 eV energy of the primary thermal electrons, but above 10 eV in deuterium. In other words, there are many more atomic neutrals in helium plasma, but the ionization is more difficult because a higher electron temperature is needed for the ionization to take place. This is confirmed by the data in figure 11(b), where

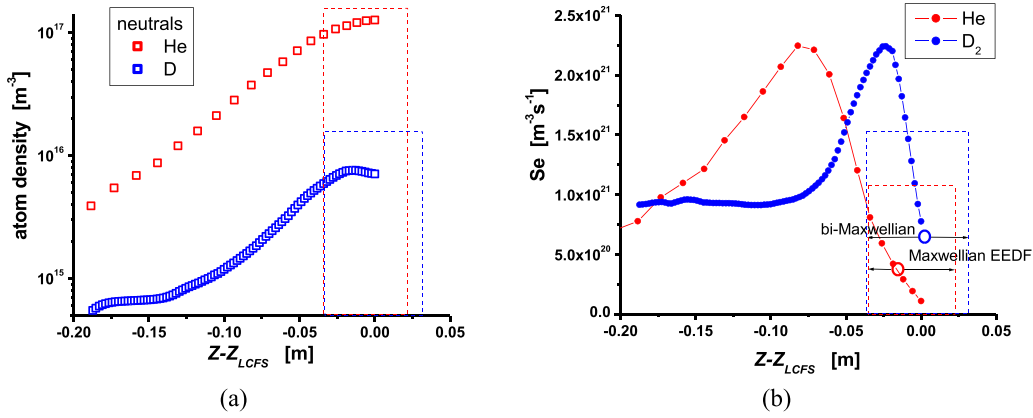


Figure 11. Radial distribution of the atom densities (a) and the electron source S_e (b) calculated by EIRENE code for deuterium (blue) and helium (red) discharges.

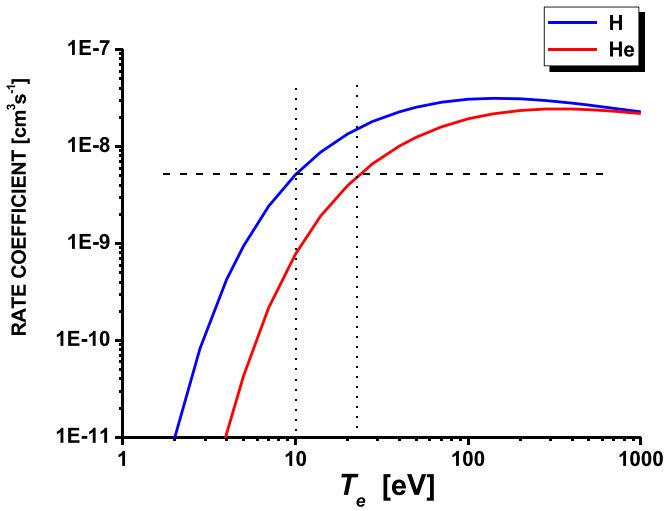


Figure 12. Ionization rate coefficient for hydrogen and helium ionization [9].

the maximum of the electron source profile is located more deeply in the confined plasma. In a deuterium plasma, ionization is easier due to the lower ionization energy. Observe that, despite the lower density of atomic neutrals (blue curve in figure 11(a)), the electron source can still be larger than in He due to the presence of molecular deuterium. Then a bi-Maxwellian appears in the vicinity of the LCFS and the plasma properties are changed.

The above results indicate that the increase in the cold electrons density is steeper than that in the thermal electrons density. It could be expected that more deeply in the plasma, before the S_e maximum in the red curve in figure 11(b), the ratio of the cold-to-thermal electron densities will be reversed as the temperature of the primary thermal electrons is increasing. It is also assumed that in the core plasma, where the electron temperature is sufficiently high, there exists a second electron source due to the ionization of He^+ —the density of He^{++} in the EIRENE code calculations is 30%–50% of the He^+ ions density.

It should be noted that not only the ionization is the responsible for the non-Maxwellian EEDF but also excitation of neutrals, which need a little lower energy of the electrons and can explain why the bi-Maxwellian in the experimental result appears, respectively for D_2 and He at 10 and 21 eV, which are lower than the ionization energies (13.6 and 24.5 eV).

In what concerns the results obtained by the experiments on the GOLEM tokamak, it is expected that when the electrons in a helium plasma are warmer (above 21 eV), a bi-Maxwellian EEDF will appear. Unfortunately, no radial measurements have so far been carried out on the WEST tokamak enabling us to process the results by applying the FDPT and analyze the electron temperature and density profiles. The first measurements in the divertor provide preliminary results in support of the validity of the hypothesis expressed here and in [5].

From the experimental side, measurements in different conditions of edge electron temperature and gas composition might help in verifying the working hypothesis. A detailed physical answer for the difference between the plasma parameters in He and D discharges could be provided by massively-parallel fully-kinetic particle-in-cell code BIT1 (1D) simulations [3], thus confirming the hypothesis of ionization of the neutrals by thermal electrons and its connection with the bi-Maxwellian EEDF.

5. Conclusions

Experiments were carried out on studying the plasma properties in the boundary region in the GOLEM tokamak and the TJ-II stellarator. The FDPT was applied to derive data for the plasma parameters from the measured I - V probe characteristics, including the EEDF, with the following results:

- In the TJ-II stellarator during the NBI heating phase in a helium plasma, the EEDF in the confined plasma is bi-Maxwellian, while close to the LCFS and in the far SOL the EEDF is Maxwellian. The electron density of the cold electrons is lower than that of the thermal ones in a helium

plasma, while the opposite holds true in a deuterium plasma. This can be explained by numerical calculations of the electron source profile, whose maximum is located more deeply in He plasma.

- The comparison of the results from probe measurements with those from EIRENE code calculations support the hypothesis that the main reason for the appearance of a bi-Maxwellian EEDF in the vicinity of the LCFS is the excitation and ionization of neutral atoms when the energy of the thermal electrons is high enough.
- The differences in the positions of appearance of a bi-Maxwellian EEDF at the different gases can be explained by the differences in the ionization rate coefficients of deuterium and helium.
- On GOLEM tokamak the experiments were only partly successful. They are compatible with the working hypothesis but cannot confirm it. The power provided is not sufficient to heat the electrons in the He discharges to temperatures exceeding 7 eV.
- In the divertor of WEST tokamak the first results show that the EEDF in the case of an almost pure He plasma is usually Maxwellian with a T_e around 17 eV. The temperature of the He plasma is not sufficiently high to observe a bi-Maxwellian distribution—production of electrons requires that the electron temperature be near He ionization potential, which exceeds 21 eV.

As conclusion, whether the non-Maxwellian EEDF appears or not depends on the working gas and the temperature of the electrons near the SOL. If there are enough neutrals and electrons hotter than the energy of the ionization for the neutrals, then the observed EEDF most probably will be non-Maxwellian.

Data availability statement

All data that support the findings of this study are included within the article (and any supplementary files).

Acknowledgments

This research was partially supported by the Joint Research Project between the Bulgarian and Czech Academies of Sciences, BAS—23-02; Contract No KP-06-N68/2 between the Bulgarian National Science Fund and the Institute of Electronics, Bulgarian Academy of Sciences and by IAEA CRP F13019—Research Contract Nos 22727, 22784 and 22782. Embie Hasan was supported by the Bulgarian Ministry of Education and Science under the National Research Programme ‘Young scientists and postdoctoral students –2’ approved by DCM 206/07.04.2022 and by Grant PID2020-116599RB-I00 funded by MCIN/AEI/10.13039/501100011033. J Kovačič acknowledges the financial support from the Slovenian Research Agency (research core Funding No. P2-0405). In Memoriam of Tsviatko Popov and Jan Stockel, who sadly passed away before the publication of this article. They both dedicated

most of their lives to electrostatic probes studies and contributed significantly to this paper.

Conflict of interest

The authors have no conflicts to disclose.

ORCID iDs

M Dimitrova  <https://orcid.org/0000-0001-6122-5172>
 D López-Bruna  <https://orcid.org/0000-0002-7638-8772>
 J Kovačič  <https://orcid.org/0000-0001-7894-9185>
 U Losada  <https://orcid.org/0000-0003-1161-8976>
 C Hidalgo  <https://orcid.org/0000-0002-0736-7855>

References

- [1] Chodura R 1992 *Contrib. Plasma Phys.* **32** 219
- [2] Batishchev O V et al 1997 *Phys. Plasmas* **4** 1672
- [3] Tskhakaya D et al 2012 *Contrib. Plasma Phys.* **52** 490
- [4] Popov T K, Ivanova P, Stöckel J and Dejarnac R 2009 *Plasma Phys. Control. Fusion* **51** 065014
- [5] Popov T K et al 2015 *Plasma Phys. Control. Fusion* **57** 115011
- [6] Jaworski M A et al 2012 *Fusion Eng. Des.* **87** 1711–8
- [7] Zhao W, Nie L, Yan L, Xu M, Ke R, Yang J, Chen Z, Wang Z and Wang Y 2021 *Plasma Sci. Technol.* **23** 035102
- [8] Dimitrova M et al 2014 *J. Phys.: Conf. Ser.* **514** 012050
- [9] Lotz W 1967 *Astrophys. J. Suppl.* **14** 207
- [10] Svoboda V, Huang B, Mlynář J, Pokol G I, Stöckel J and Vondrášek G 2011 *Fusion Eng. Des.* **86** 1310–4
- [11] Hidalgo C et al 2022 *Nucl. Fusion* **62** 042025
- [12] Bucalossi J et al 2022 *Nucl. Fusion* **62** 042007
- [13] Demidov V I et al 1996 *Probe Methods for Low-Temperature Plasma Investigations* (Energoatomizdat) (in Russian)
- [14] Popov T K, Dimitrova M, Ivanova P, Kovačič J, Gyergyek T, Dejarnac R, Stöckel J, Pedrosa M A, López-Bruna D and Hidalgo C 2016 *Plasma Sources Sci. Technol.* **25** 033001
- [15] Druyvesteyn M J 1930 *Z. Phys.* **64** 781
- [16] Swift J D 1962 *Proc. Phys. Soc.* **79** 697
- [17] Malkov M A 1991 *High Temp.* **29** 329–35 (available at: www.mathnet.ru/php/archive.phtml?wshow=paper&jrmid=tv&paperid=4231&option_lang=engCitation)
- [18] Arslanbekov R R, Khromov N A and Kudryavtsev A A 1994 *Plasma Sources Sci. Technol.* **3** 528
- [19] Rozhansky V and Tsengin L 2001 *Transport Phenomena in Partially Ionized Plasma* (Gordon and Breach)
- [20] Demidov V I, Ratynskaia S V, Armstrong R J and Rypdal K 1999 *Phys. Plasmas* **6** 350
- [21] Popov T K, Ivanova P, Dimitrova M, Kovačič J, Gyergyek T and Čerček M 2012 *Plasma Sources Sci. Technol.* **21** 025004
- [22] Popov T et al 2006 *J. Phys.: Conf. Ser.* **44** 60
- [23] Demidov V I, Ratynskaia S V and Rypdal K 2001 *Contrib. Plasma Phys.* **41** 443
- [24] Rypdal K, Gronvoll E, Oynes F, Fredriksen A, Armstrong R J, Trulsen J and Pecceli H L 1994 *Plasma Phys. Control. Fusion* **36** 1099
- [25] Stangeby P C 1982 *J. Phys. D: Appl. Phys.* **15** 1007
- [26] Demidov V I, Ratynskaia S V and Rypdal K 2002 *Rev. Sci. Instrum.* **73** 3409
- [27] Golant V E et al 1980 *Fundam. Plasma Phys.* (Wiley)
- [28] Kaufman H R 1990 *J. Vac. Sci. Technol. B* **8** 107
- [29] Stangeby P C 1995 *Plasma Phys. Control. Fusion* **37** 1337

- [30] Dimitrova M, Dejarnac R, Popov T K, Ivanova P, Vasileva E, Kovačič J, Stöckel J, Havlicek J, Janky F and Panek R 2014 *Contrib. Plasma Phys.* **54** 255
- [31] Popov T K, Dimitrova M, Ivanova P, Hasan E, Horáček J, Dejarnac R, Stöckel J, Weinzettl V and Kovačič J 2014 *Contrib. Plasma Phys.* **54** 267
- [32] López-Bruna D *et al* 2016 *J. Phys.: Conf. Ser.* **700** 012006
- [33] Svoboda V, Zhekova M, Dimitrova M, Marinova P, Podolník A and Stockel J 2019 *J. Fusion Energy* **38** 253–61
- [34] Desideri D and Serianni G 1998 *Rev. Sci. Instrum.* **69** 2354
- [35] Dejarnac R, Gunn J P, Stöckel J, Adámek J, Brotánková J and Ioniþá C 2007 *Plasma Phys. Control. Fusion* **49** 1791
- [36] Hasan E *et al* 2018 *J. Instrum.* **13** P04005
- [37] Dejarnac R, Sestak D, Gunn J P, Firdaouss M, Greuner H, Pascal J-Y, Richou M and Roche H 2021 *Fusion Eng. Des.* **163** 112120
- [38] Bisson R *et al* 2021 *Nucl. Mater. Energy* **26** 100885
- [39] Castejón F *et al* 2017 *Nucl. Fusion* **57** 102022